International Journal of Heat and Mass Transfer 121 (2018) 1168–1178

Contents lists available at ScienceDirect

International Journal of Heat and Mass Transfer

journal homepage: www.elsevier.com/locate/ijhmt

MHD natural convection flow enclosure in a corrugated cavity filled with a porous medium

Rizwan Ul Haq [a], Feroz Ahmed Soomro [b], Toufik Mekkaoui [c], Qasem M. Al-Mdallal [d,*]

[a] Department of Electrical Engineering, Bahria University, Islamabad 40000, Pakistan
[b] Department of Mathematics, Nanjing University, Nanjing 210093, China
[c] Equipe E3MI, D'epartement de Math'ematique, FST Errachidia, Universit'e Moulay Ismail, BP.509, Boutalamine, 52000 Errachidia, Morocco
[d] Department of Mathematical Sciences, United Arab Emirates University, Al-Ain, United Arab Emirates

ARTICLE INFO

Article history:
Received 19 November 2017
Received in revised form 10 January 2018
Accepted 14 January 2018

Keywords:
Natural convection
Corrugated cavity
Porous medium
Finite element method
MHD

ABSTRACT

In this article, a complete structure of corrugated surface is established for heat transfer effects in the presence of uniform magnetic field. A natural convection phenomenon is presented for MHD flow filled in a porous corrugated cavity at various wavelengths and partially heated domain. The governing partial differential equations consist of continuity, momentum and energy equations along with the corrugated conditions at the surface. This system is properly nondimensionalized and then solved via finite element method (FEM). In order to obtain the high resolution near the surface of corrugation, mesh generation is improved at the various portions of the cavity. The flow patterns and temperature distribution within the entire domain of the cavity can be visualized through streamlines and isotherms, respectively. Computational experiment is performed for various values of wavelength number $(0 \leqslant n \leqslant 15)$, Rayleigh number $(10^4 \leqslant Ra \leqslant 10^6)$, Darcy number $(10^{-5} \leqslant Da \leqslant 10^{-3})$, and Hartmann number $(10 \leqslant Ha \leqslant 10^3)$ to illustrate the effects on streamlines, isotherms, velocities and heat transfer rate. Heat transfer rate is increased due to increase in Rayleigh number and wavelength parameter. Darcy and Hartmann number does not have significant effects on the temperature distribution.

1. Introduction

Apart from daily use, natural convection is the type of heat transfer phenomenon that is used in many industrial processes for better performances, aerodynamics, including energy, heat transfer, light–thermal conversion and other performances. Different from the forced convection, natural convection can occur due to the density difference where the buoyancy forces uplift the low-density fluid (high temperature fluid) and drops down the high density fluid (low temperature fluid). This subject is very crucial to address due to readily applications. The study of natural convection in enclosures helps in manufacturing the best suitable windows with feasible glass panels which saves allot of energy due to resistance of outer temperature come inside and vice versa. Besides, it has tremendous other engineering application too, such as cooling and heating of houses, solar collectors, cooling of electric devices, to micro-electromechanical systems (MEMS), food processing, metallurgical industry are few of them. For detailed analysis on the applications the readers are referred to [1–3].

Contrary to the flow problems in open channels, the flow and heat transfer problems in enclosed cavity are not that simple. There are many obstacles among which geometry shape, boundary conditions, type of governing equations and thus seeking the best numerical solution are few of them. This important field of research has owned tremendous importance due to its inevitable applications. Such applications include heating/cooling of houses, microprocessors, air conditioning, solar collectors and so on. The researchers' quest has always been to enhance the performance of such processes. We may find large amount of literature addressing these important physical problems. Both experimental and mathematical studies were carried out by many researchers. We will refrain from experimental infestations and only give sufficient background of the mathematical studies. For example, a mathematical analysis on the buoyancy-driven flow and heat transfer of nanofluid flow was done numerically using finite volume method [4]. The flow was confined to the two-dimensional rectangular enclosure. In another study the flow and heat transfer governed by lid-driven cavity with differentially heated side wall was studied numerically using SIMPLE algorithm [5]. A detailed

* Corresponding author.
E-mail addresses: ideal_riz@hotmail.com (R.U. Haq), q.almdallal@uaeu.ac.ae (Q.M. Al-Mdallal).

https://doi.org/10.1016/j.ijheatmasstransfer.2018.01.063
0017-9310/

analysis on the effects of pertinent parameters on the heat transfer rate as well as on streamlines and isotherms were reported. Abu-Nada and Oztop [6] considered the inclined square cavity to study the natural convection heat transfer. Effects of various angles of inclinations on the flow and heat transfer characteristics were analyzed. Finite Volume method was used to seek the numerical solution.

Various kinds of cavity shapes exist in the engineering applications. For example, triangular cavity [7–9], rectangular cavity [5,10–12], trapezoidal cavity [13–15], and other shaped cavities [16–19]. Cavity with corrugated walls is another kind of interesting geometry whose application lies in solar collectors, designing of house roof to make the house cold or hot, etc. Recently, various researchers have taken various shapes of cavities to analyze the effects of corrugated wall geometry on the natural and forced convection heat transfer. Shivan et al. [20] studied the natural convection flow inside the square cavity with one side wall cosine corrugated. Triangular cavity with bottom corrugated wall was considered by Rahman et al. [21]. The effects of corrugated wall on the natural convection heat transfer of nanofluid flow were analyzed in detail using Buongiorno's model. In another study [22] the effects of increasing number of corrugation frequency on the natural convection heat transfer were studied numerically using finite element method. Above cited references are all geometries with any one wall corrugated. The square cavity with two side corrugated walls was taken into consideration by Hasan et al. [23] to study the heat transfer characteristics of natural convection flow. Horizontal channel with upper and lower corrugated wall was considered by Jafri et al. [24]. SWCNT suspended nanofluid with base fluid water was used as working fluid to study the heat transfer management. Numerical solution was obtained using Lattice Boltzmann Method.

In the present study, we incorporate porous medium inside the cavity. Such kind of cavity exists in the variety of fields including filtration, construction, soil mechanics, biophysics, and so on. The porous medium may greatly affect the heat transfer rate. The study would be useful in optimizing the energy usage and other benefits. Literature search reveals that the problem has remained a hot topic among the researchers who have studied the flow and heat transfer through porous medium in both open [25] and closed regions [26–28]. Moreover, both conventional fluids and nanofluids have been utilized during such diverse studies. Present study will stick to the cavity flow with conventional fluid. Nithiarasu et al. [29] studied numerically the natural convection flow through the porous medium. The results were validated with reported experimental results. In another study [30] the flow through the wavy vertical cavity filled with porous medium was considered. The solution was obtained numerically using Finite Element Method. Sheremet et al. [31] incorporated nanofluid in the Buongiorno's model to study the three-dimensional natural convection heat transfer in a cubical cavity filled with porous medium. Tariq et al. [32] took into consideration the non-Newtonian MHD nanofluid to study the effects of porous medium on the mixed convection inside the triangular cavity. Upper corrugated rectangular cavity filled with porous medium was considered by Sheikholeslami and Shamlooei [33]. The study revealed that incorporation of porous medium enhanced heat transfer rate. The interesting geometry of differentially heated square cavity with aspiration was studied by Biswas and Manna [34]. The study revealed that the flow and heat transfer was greatly affected by the range of porosity parameter. Apart from mentioned studies, various effects to determine the heat transfer rate for various geometries [35–39].

So, the main feature of the present article is to numerically investigate the natural convection flow of magnetohydrodynamic fluid inside the corrugated cavity filled with porous medium. The distribution of article is as follows: the introduction section 1 gives the brief background of the problem and sets the motivation to carryout present piece of research work. Modeling of problem and its mathematical formulation is given in Section 2. Numerical procedure to solve the governing partial differential equations using finite element method is defined in the Section 3. Detailed analysis on the obtained results has been given in Section 4. Major interesting results obtained in the present study are summarized in the conclusion Section 5. All the cited references are listed in the last section of references.

2. Description of physical problem

Consider two dimensional MHD viscous fluid saturated porous medium enclosed in a rectangular shape cavity with bottom and top surfaces are corrugated while other two vertical walls are smooth. It is further assumed that temperature of both solid phase and fluid phase are uniform for porous medium. Moreover, state of fluid's molecules is in the form of local thermal equilibrium for given model. Since we are dealing the natural convection phenomena in a cavity therefore velocity square effects can be discarded for present model. In cartesian coordinate system (XY – plane), U and V are velocity components along X and Y – direction respectively (see Fig. 1).

2.1. Constraint at walls

In order to define the boundary conditions at the entire walls of the cavity, first we fixed all the velocities at the surfaces are zero.

$$\begin{cases} T^*\left(X, Y = aSin\left(n\pi\frac{X}{L}\right)\right) = T_h \\ \quad \text{for } 0 \leqslant X \leqslant L, \text{ Temperature at lower corrugated surface} \\ \frac{\partial T^*\left(X, Y = \frac{L}{2} + aSin\left(n\pi\frac{X}{L}\right)\right)}{\partial Y} = 0 \\ \quad \text{for } 0 \leqslant X \leqslant L, \text{ Temperature at upper corrugated surface} \end{cases}$$

Temperature at vertical walls is kept cold:

$$T^*(X = 0, Y) = T^*(X = 1, Y) = T_c \text{ for } 0 \leqslant Y \leqslant \frac{L}{2}.$$

Velocities at all solid boundaries $U = V = 0$. In the above mention conditions, X, Y are the space variables, a is the amplitude, n is the wavelength number.

2.2. Governing equations

For present model, we have considered a steady, MHD, viscous, incompressible flow in xy – coordinate system. Further we are considering that channel is filled with porous medium and motion of the fluid depending upon Darcy's law, which produce for the drag exerted by the porous medium. The viscous dissipation effect is neglected and system of governing partial differential equation depends upon continuity equation under the law of conservation of mass, momentum and energy equations:

$$\frac{\partial U}{\partial X} + \frac{\partial V}{\partial Y} = 0, \tag{1}$$

$$\rho\left(U\frac{\partial U}{\partial X} + V\frac{\partial U}{\partial Y}\right) = -\frac{\partial P}{\partial X} + \mu\left(\frac{\partial^2 U}{\partial X^2} + \frac{\partial^2 u}{\partial y^2}\right) - \frac{\mu}{K}U, \tag{2}$$

$$\rho\left(U\frac{\partial V}{\partial X} + V\frac{\partial V}{\partial Y}\right) = -\frac{\partial P}{\partial Y} + \mu\left(\frac{\partial^2 V}{\partial X^2} + \frac{\partial^2 V}{\partial y^2}\right) - \frac{\mu}{K}V - \sigma B_0^2 V + g\rho\beta(T^* - T_c) \tag{3}$$

$$\left(U\frac{\partial T^*}{\partial x} + V\frac{\partial T^*}{\partial y}\right) = \alpha\left(\frac{\partial^2 T^*}{\partial x^2} + \frac{\partial^2 T^*}{\partial y^2}\right). \tag{4}$$

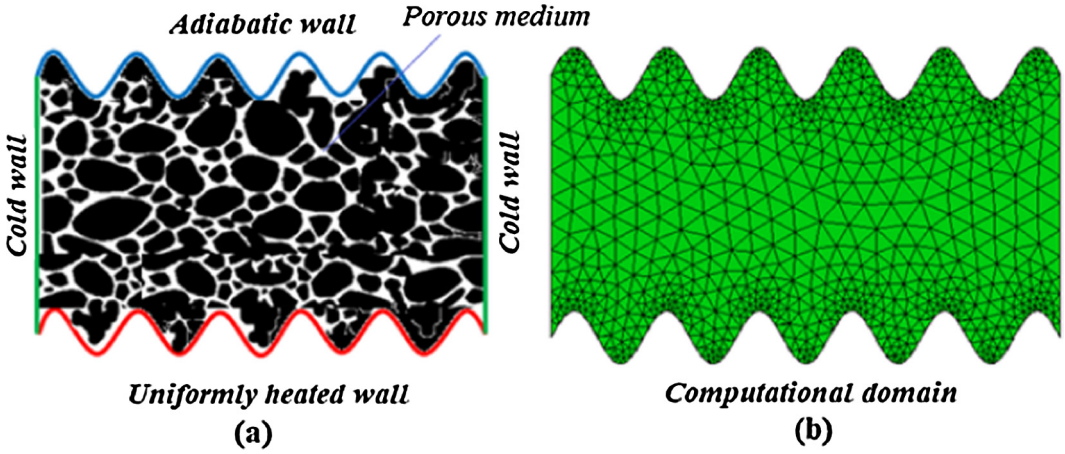

Fig. 1. Geometry of the model (a) physical domain and (b) computational domain.

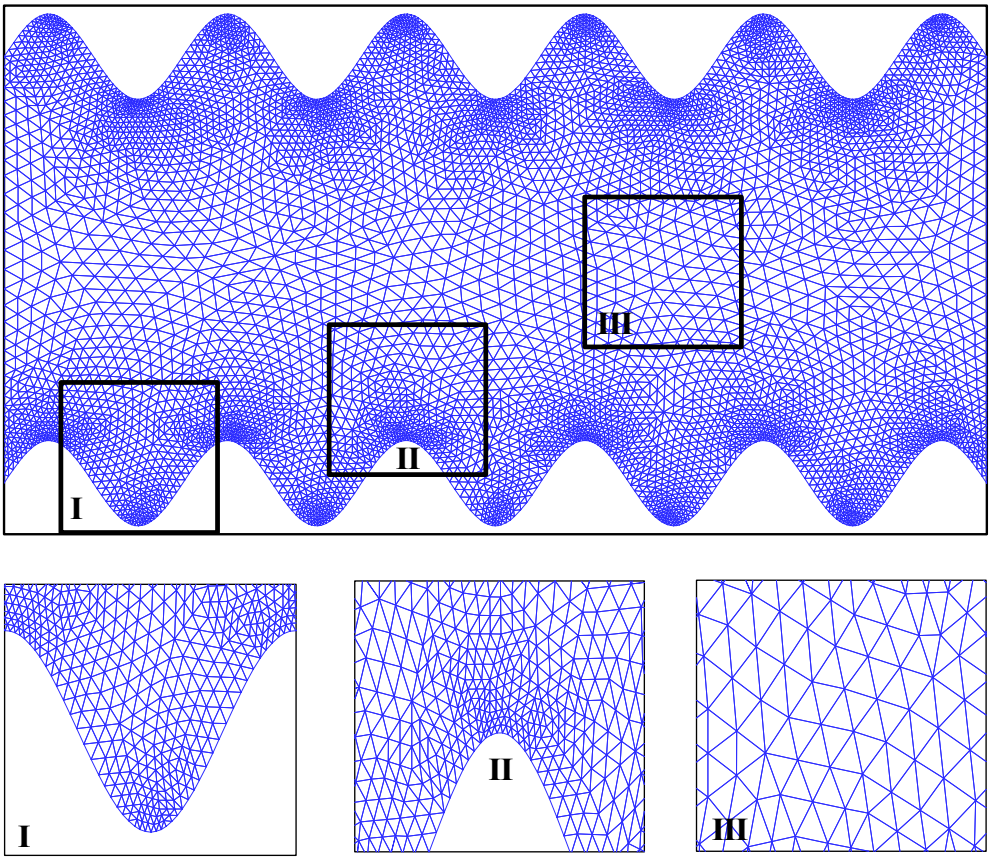

Fig. 2. Mesh analysis at different portion of the corrugated cavity.

In the above system of equations, U and V are the velocities along X and Y-directions, respectively. Where, T^* is the temperature of the fluid and P is the pressure of the fluid. The dimensionless quantities are:

$$x=\frac{X}{L},\quad y=\frac{Y}{L},\quad u=\frac{UL}{\alpha},\quad v=\frac{VL}{\alpha},\quad T=\frac{T^*-T_c}{T_h-T_c},\quad p=\frac{PL^2}{\rho\alpha^2},\quad v=\frac{\mu}{\rho}.$$

Invoking the dimensionless variable in Eqs. (1)–(4), we get:

$$u\frac{\partial u}{\partial x}+v\frac{\partial u}{\partial y}=-\frac{\partial p}{\partial x}+Pr\left(\frac{\partial^2 u}{\partial x^2}+\frac{\partial^2 u}{\partial y^2}\right)-\frac{Pr}{Da}u, \tag{5}$$

$$u\frac{\partial v}{\partial x}+v\frac{\partial v}{\partial y}=-\frac{\partial p}{\partial y}+Pr\left(\frac{\partial^2 v}{\partial x^2}+\frac{\partial^2 v}{\partial y^2}\right)+PrRaT-(Ha)^2Prv-\frac{Pr}{Da}v, \tag{6}$$

$$\left(u\frac{\partial T}{\partial x}+v\frac{\partial T}{\partial y}\right)=\left(\frac{\partial^2 T}{\partial x}+\frac{\partial^2 T}{\partial y}\right). \tag{7}$$

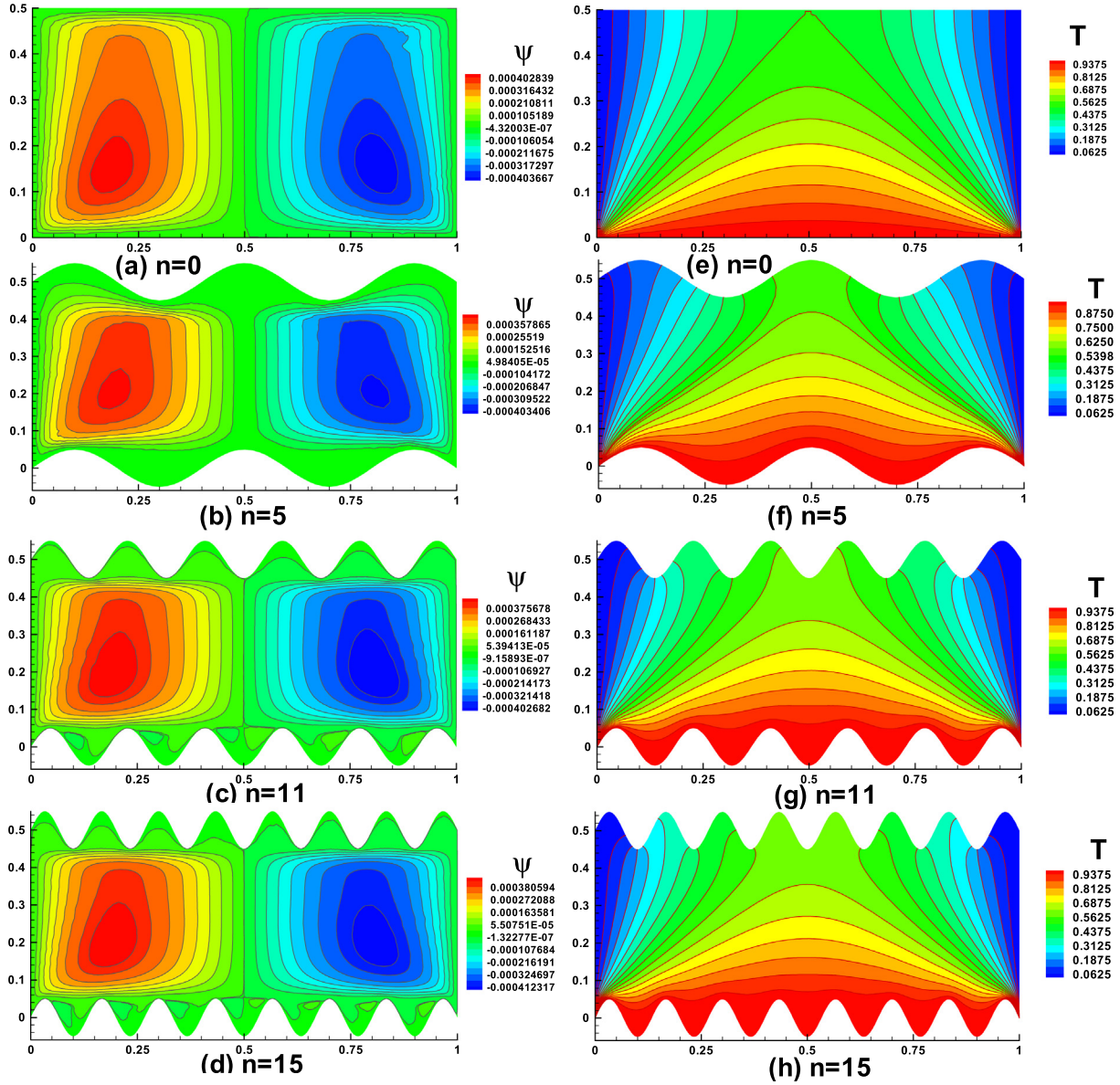

Fig. 3. Variation of (a)–(d) stream function and (e)–(h) isotherms for various values of wavelength number n when $Ra = 10^4, Da = 10^{-4}, Pr = 6.2, Ha = 10^3$.

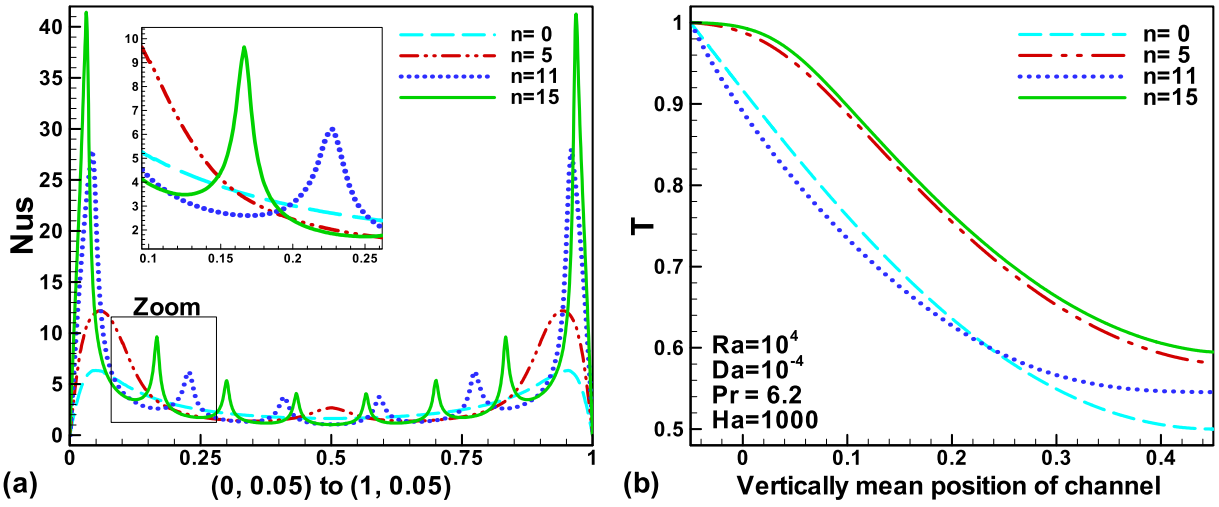

Fig. 4. Variation of (a) Nusselt and (b) temperature for various values of wavelength number n when $Ra = 10^4, Da = 10^{-4}, Pr = 6.2$ and $Ha = 10^3$.

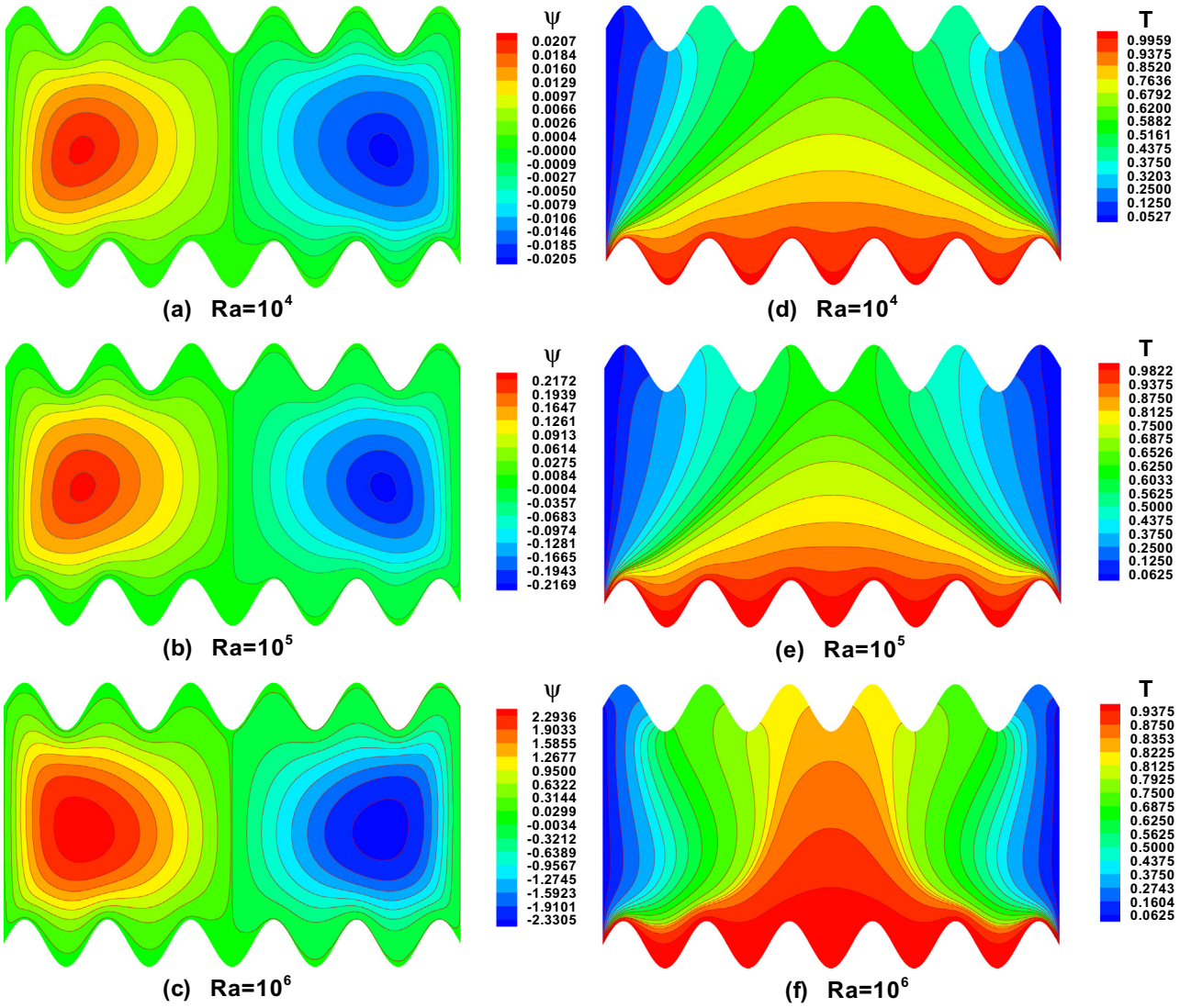

Fig. 5. Variation of (a)–(c) stream function and (d)–(f) isotherms for various values of Rayleigh number Ra when $Da = 10^{-4}$, $Pr = 6.2$ and $Ha = 10$.

In the above system of equations, the dimensionless parameters are defined as:

$$Pr = \frac{\upsilon}{\alpha}, \quad Ra = \frac{g\beta(T_h - T_c)L^3}{\upsilon\alpha}, \quad Da = \frac{K}{L^2}, \quad Ha = B_o L\sqrt{\frac{\sigma}{\mu}}.$$

In the above equations, Pr, Ra, Da and Ha are Prandtl number, Rayleigh number, Darcy numbers and Hartmann number, respectively. The dimensionless form of associated boundary conditions for entire domain is defined as:

$$\begin{cases} T\left(x, y = \frac{Sin(n\pi x)}{\lambda}\right) = 1 \\ \quad \text{for } 0 \leqslant x \leqslant 1, \text{ temperature at lower corrugated surface.} \\ \frac{\partial T\left(x, y = 0.5 + \frac{Sin(n\pi x)}{\lambda}\right)}{\partial y} = 0 \\ \quad \text{for } 0 \leqslant x \leqslant 1, \text{ temperature at upper corrugated surface.} \end{cases} \tag{8a}$$

Temperature at vertical walls is kept cold:

$$T(0, y) = T(1, y) = 0 \text{ for } 0 \leqslant y \leqslant 0.5, \tag{8b}$$

Velocities at all solid boundaries $u = v = 0$. (8c)

In Eq. 8(a), $\lambda = L/a$ is the amplitude ratio.

Average Nusselt number along a partially heated domain of enclosure is defined as:

$$Nu_{avg} = \int_S -\left(\frac{dT}{dn}\right) dX. \tag{9}$$

where "n" is normal direction at the surface of corrugated along the heated surface (S).

2.3. Impact of wavelength n

Before going to analyze the entire results, it is important to note that our model is strongly depending upon wavelength number n and amplitude ratio λ. Throughout the results, amplitude ratio is fixed that is ($\lambda = 20$). However, we have checked the variation of stream function and isotherms at various wave lengths with respect to $n = 0, n = 5, n = 11$ and $n = 15$ (see Figs. 3 and 4). However, for the rest of the results we have fixed the wavelength for $n = 11$. It is important to note that for $n = 0$ present corrugated surfaces will produce the results for flat rectangular shape cavity.

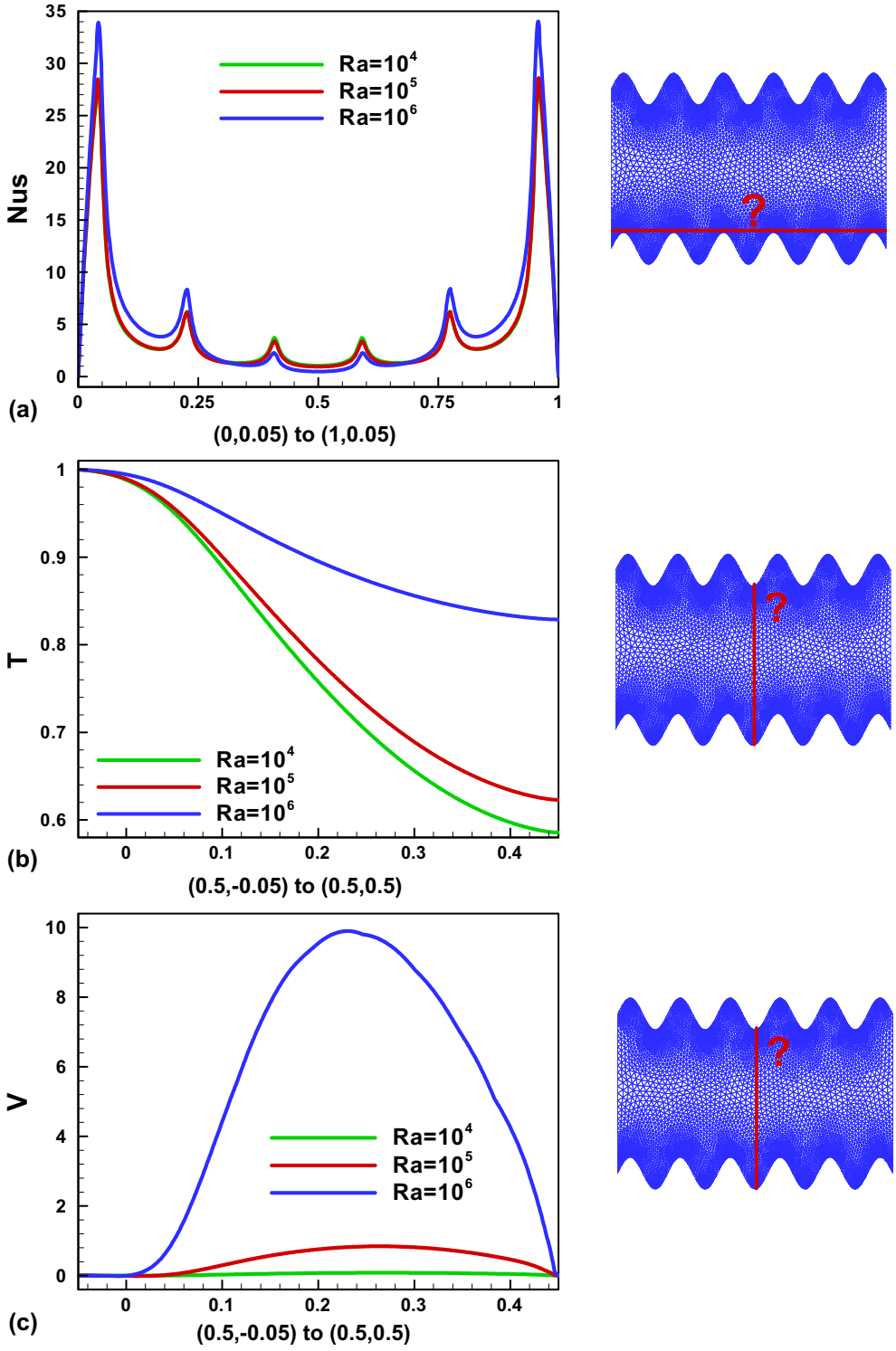

Fig. 6. Variation of (a) Nusselt number, (b) temperature and (c) velocity v in the described domain for various values of Ra when $Da = 10^{-4}$, $Pr = 6.2$ and $Ha = 10$.

3. Methodology

The set of Eqs. (5)–(7) along with boundary conditions (8) are solved using finite element method using Galerkin approach. Non-uniform triangular elements mesh is used for discretization of domain. Moreover, we have considered much dense mesh at the typical points (see Fig. 2). The pressure term (P) is eliminated via continuity equation using the constraint equation $p = -\gamma\left(\frac{\partial u}{\partial x} + \frac{\partial v}{\partial y}\right)$. The continuity Eq. (1) identically satisfied for highly greater value that is $\gamma = 10^7$. By replacing the pressure p, terms in Eqs. (5) and (6) we get:

$$\left(u\frac{\partial u}{\partial x} + v\frac{\partial u}{\partial v}\right) = \gamma\frac{\partial}{\partial x}\left(\frac{\partial u}{\partial x} + \frac{\partial v}{\partial y}\right) + Pr\left(\frac{\partial^2 u}{\partial x^2} + \frac{\partial^2 u}{\partial y^2}\right) - \frac{Pr}{Da}u, \qquad (10)$$

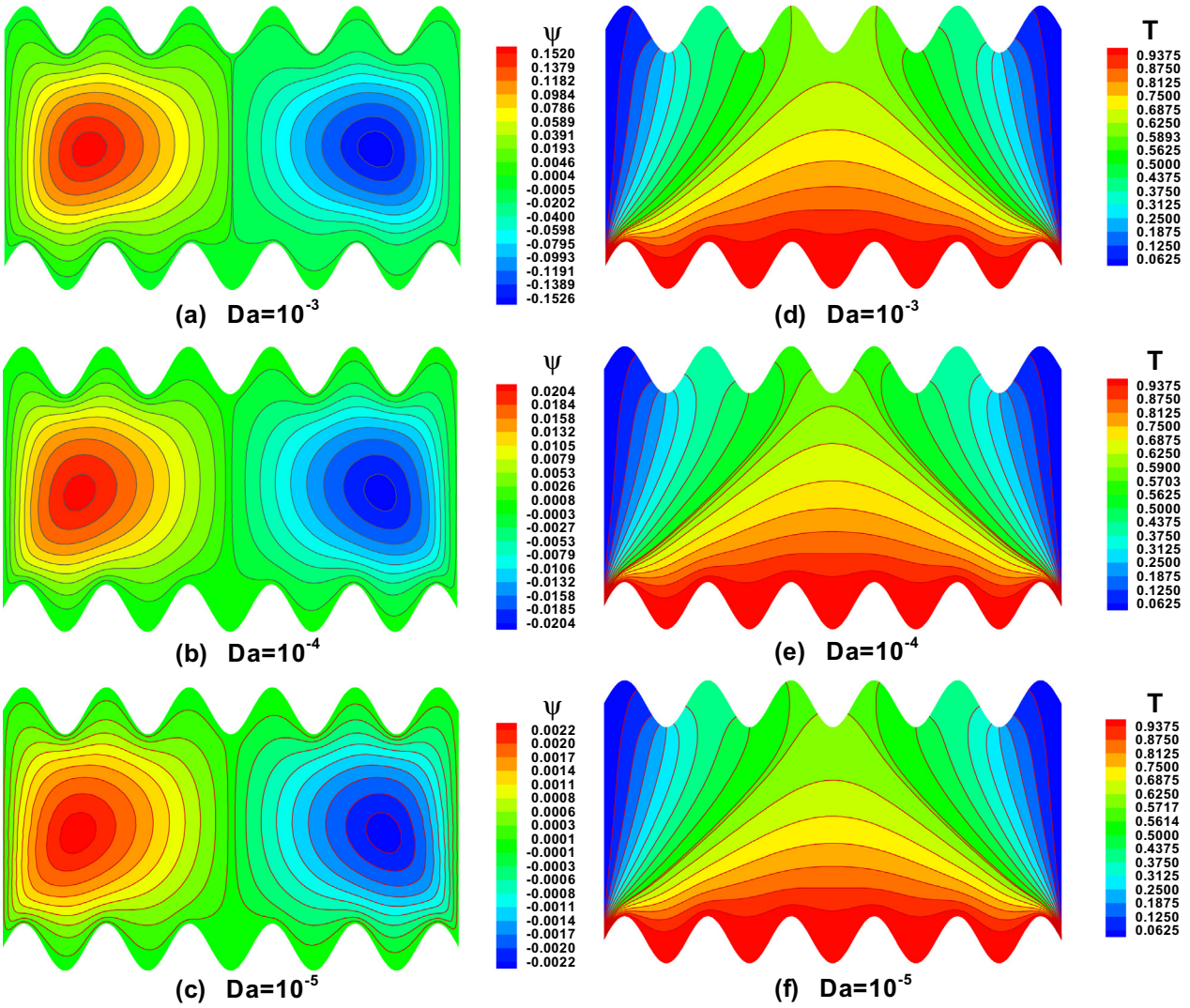

Fig. 7. Variation of (a)–(c) stream function and (d)–(f) isotherms for various values of Darcy number when $Ra = 10^4, Pr = 6.2$ and $Ha = 10$.

And similarly

$$u\frac{\partial v}{\partial x} + v\frac{\partial v}{\partial y} = \gamma\frac{\partial}{\partial y}\left(\frac{\partial u}{\partial x} + \frac{\partial v}{\partial y}\right) + Pr\left(\frac{\partial^2 v}{\partial x^2} + \frac{\partial^2 v}{\partial y^2}\right) + \mathrm{Pr}RaT - (Ha)^2\mathrm{Pr}\ v - \frac{\mathrm{Pr}}{Da}v, \tag{11}$$

For detailed procedure, readers are referred to the article of Taylor and Hood [40] and book of Dechaumphai [41]. While implemented the methodology, it is important to check the accuracy and efficiency of all results. For this, increment of elements at upper and lower surface of the corrugation are added to enhance the accuracy and better convergence (see Fig. 2).

4. Results and discussion

The magnetohydrodynamic natural convection fluid flow inside the corrugated cavity filled with porous medium has been investigated numerically using finite element method. The geometry of the cavity is considered as rectangle where the lower and upper wall is corrugated with uniformly heated and adiabatic, respectively, whereas other two side walls are kept at comparatively cold temperature. The numerical experiment was performed for various values of wavelength parameter ($0 \leqslant n \leqslant 15$), Rayleigh number ($10^4 \leqslant Ra \leqslant 10^6$), Darcy number ($10^{-5} \leqslant Da \leqslant 10^{-5}$) and Hartmann number ($10^2 \leqslant Ha \leqslant 10^3$) on the fluid velocity, flow patterns, temperature distribution and heat transfer rate. Flow patterns and temperature distribution are shown graphically using streamlines and isotherms plots. The results are concluded into the subsequent paragraphs.

4.1. Effects of wave length parameter

Fig. 3 presents the effects of wavelength parameter on the streamlines and isotherms. It is evident from the Fig. 3(a)–(d) that the flow strength gets stronger by increasing the wavelength parameter. The streamlines occupy the whole cavity with the increase in wavelength parameter. On the other hand, increasing the number of wavelength parameter distributes more heat to the surrounding as it can be seen from the isotherms Fig. 3(e)–(h). The heat starts to spread out from the mid-section of the cavity towards upper wall which is due to the vertical cold walls. In whole range of wavelength parameter, the temperature of bottom wall remains higher comparatively to upper wall due to the fact that lower corrugated wall is uniformly heated whereas upper wall is adiabatic. This phenomenon can be seen from Fig. 4(b) which shows the temperature profiles along the vertical mean path

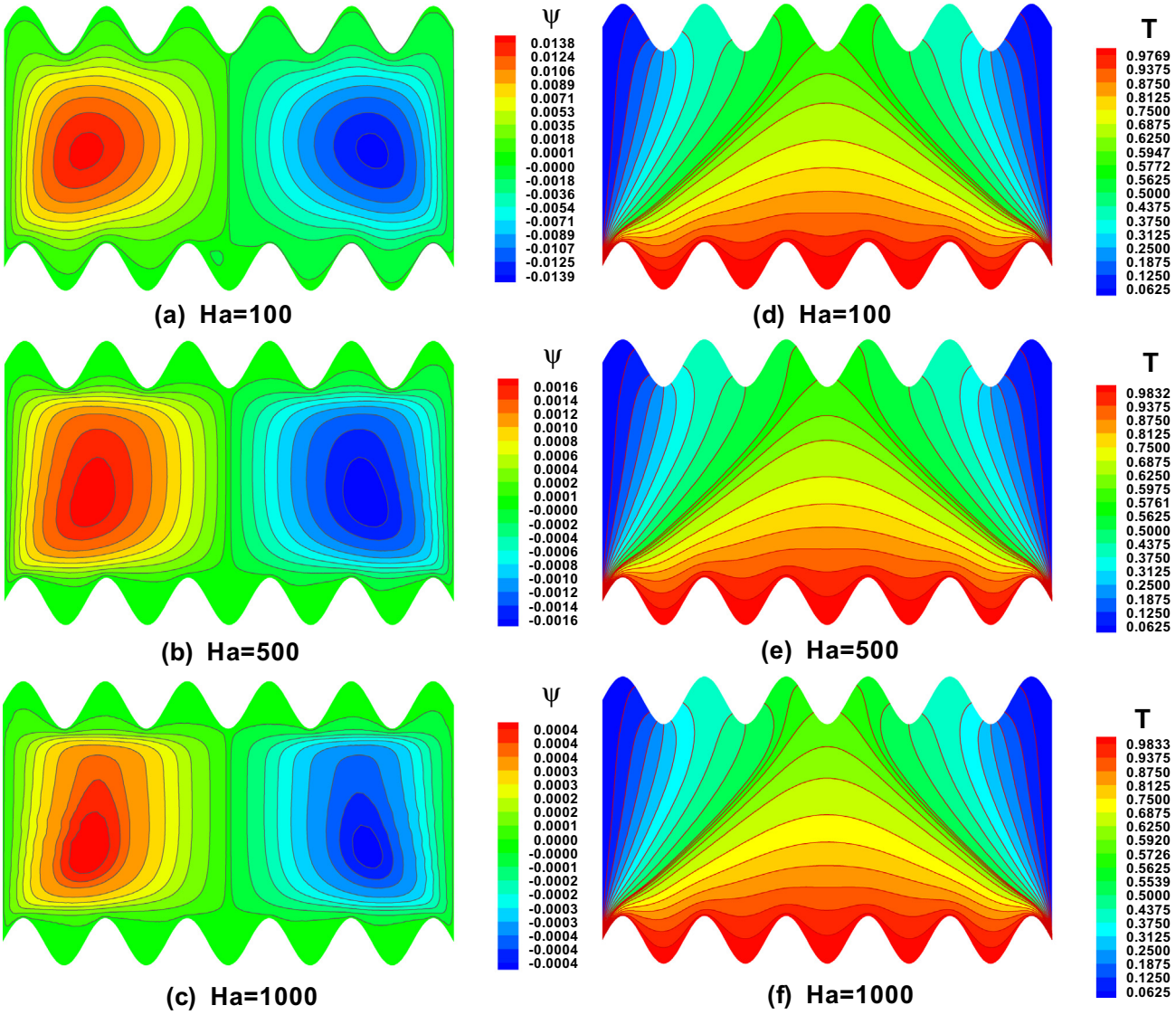

Fig. 8. Variation of (a)–(c) stream function and (d)–(f) isotherms for various values of Hartmann number when $Ra = 10^4, Pr = 6.2$ and $Da = 10^{-4}$.

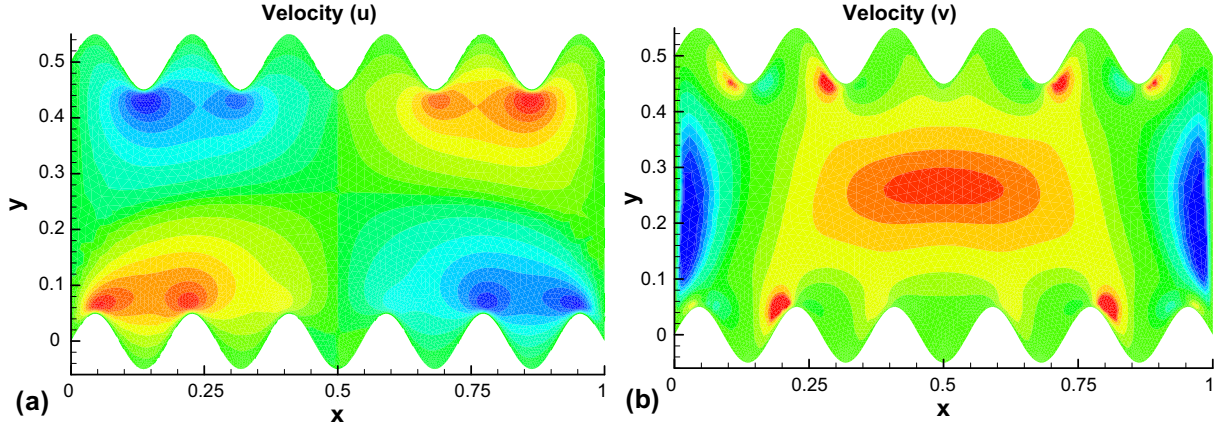

Fig. 9. Variation of (a) velocity u and (b) velocity v when $Ra = 10^4$, $Da = 10^{-4}$, $Pr = 6.2$ and $Ha = 10$.

(0.5, 0) to (0.5, 0.4) of the cavity. The profiles further disclose that the temperature of the fluid at the upper mean position tends to increase due to increase in wavelength parameter which clearly supports the trends observed in Fig. 3(e)–(h). Fig. 4(a) shows the rate of heat transfer along horizontal path near to the corrugated surface between (0, 0.05) to (1, 0.05). A corrugated shape behavior

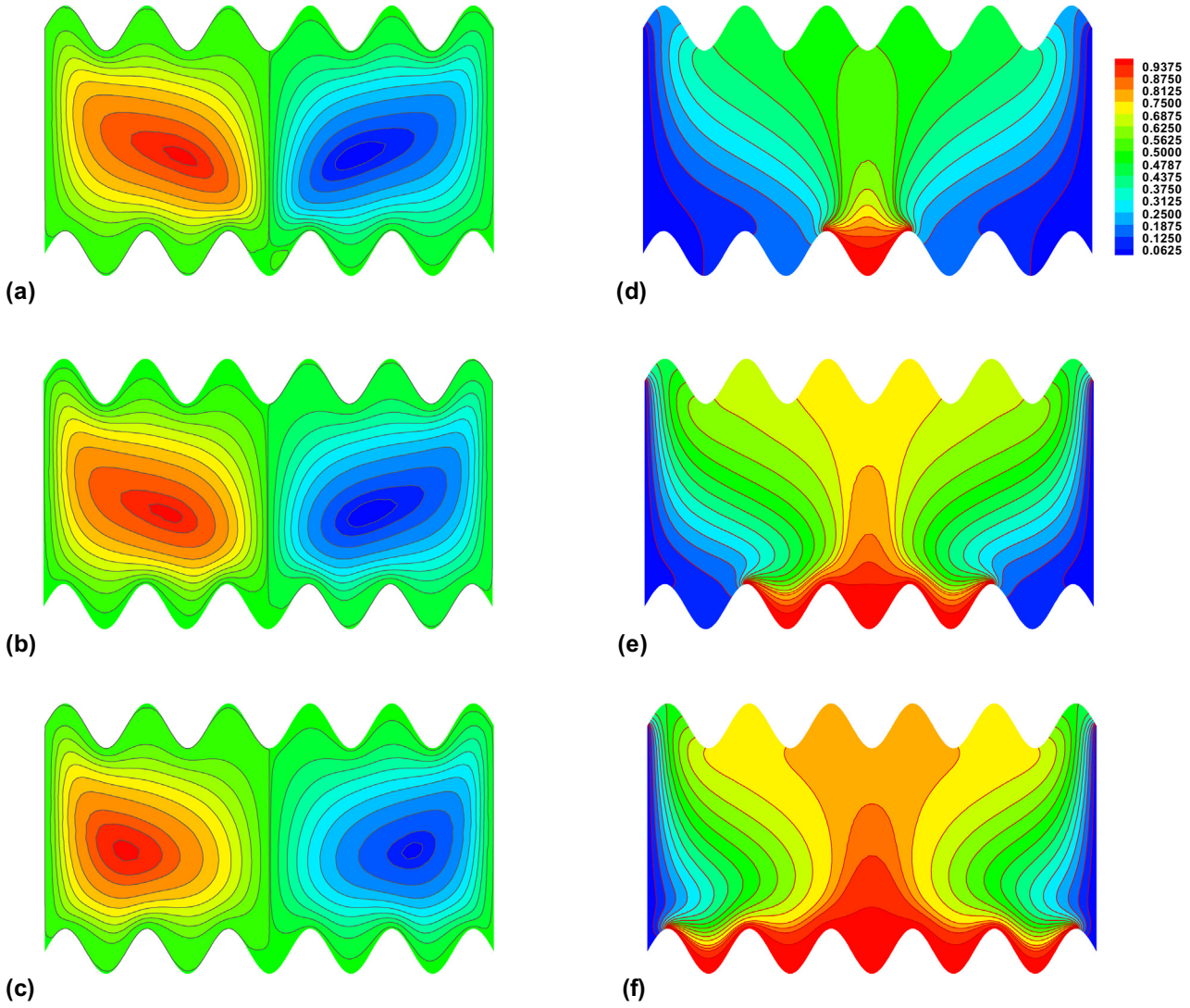

Fig. 10. Variation of (a)–(c) stream function and (d)–(f) isotherms for various heated lengths of the corrugated cavity when $Ra = 10^{6.5}, Pr = 6.2, Ha = 10$ and $Da = 10^{-4}$.

is observed due to the high intensity of heat the surface and it varies with respect to the shape of corrugation. It is evident from the profiles that there is maximum heat transfer rate at the two ends of the cavity due to the vertical cold walls. Moreover, it is noticed that heat transfer rate is increased due to increase in wavelength parameter.

4.2. Effects of Rayleigh number

Fig. 5 shows the effects of Rayleigh number on the streamlines and isotherms. It can be seen clearly that the flow currents become strong as we increase the Rayleigh number. At $Ra = 10^6$ the flow lines occupy whole cavity with strong flow currents. The temperature of the cavity also tends to increase when we increase Rayleigh number. Due to side cold walls the temperature of the fluid tends to spread through the mid vertical section. Fig. 6 shows the profiles of heat transfer rate, temperature distribution and velocity along the defined mean path. The heat transfer rate is maximum at two ends of the cavity due to vertical cold walls. Moreover, it is evident from the profile trends that heat transfer rate tend to increase with increase in Rayleigh number. Temperature of the fluid tends to increase due to increase in Rayleigh number. On the other hand, it tends to decrease along the vertical mean path. It is clear from the profiles that the rate of dropping temperature is higher for low Rayleigh number as compared to high Rayleigh number. Fig. 6(c) shows the velocity profiles against different values of Rayleigh number along the vertical mean path. It can be clearly seen that the velocity tends to increase due to increase in Rayleigh number and the maximum velocity is obtained at the mid-section of the vertical mean path.

4.3. Effects of Darcy number

Effect of porosity on the velocity and temperature fields are depicted in Fig. 7 using streamlines (a)–(c) and isotherm (d)–(f) plots. Decreasing value of Darcy parameter produces increase in the velocity strength. It can be seen from Fig. 7(a)–(c) that the streamlines tend to get strong and occupy the whole cavity as the Darcy parameter is decreased from 10^{-3} to 10^{-5}. Moreover, it does not have significant effects on the temperature distribution for the considered range of Darcy parameter.

4.4. Effects of Hartmann number

Fig. 8 shows the streamlines and isotherm plots against the increase value of Hartman number. Increasing the magnetic field

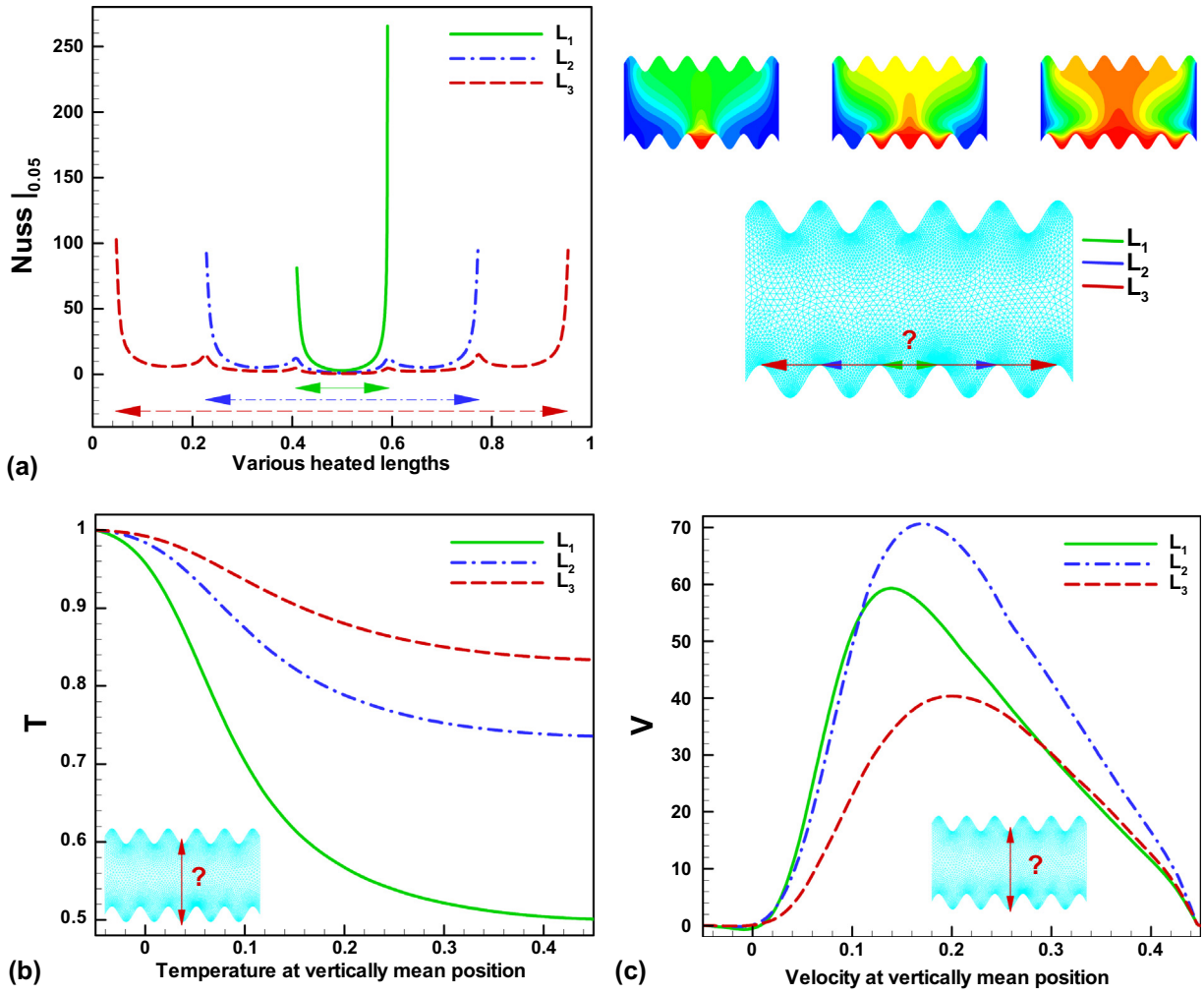

Fig. 11. Variation of (a) Nusselt number, (b) temperature and (c) velocity v in the described domain for various heated lengths of the corrugated cavity when $Ra = 10^{6.5}$, $Pr = 6.2$, $Ha = 10$ and $Da = 10^{-4}$.

effects produces increase in streamline strength. The interesting fact is that it does not occupy the whole cavity at comparatively large Hartmann number. The flow cells converge to their own center. On the other hand, it does not have significant effects on the temperature distribution for considered range of Hartman number.

4.5. Velocity profiles

Since it is important to identify the behavior of the fluid molecules along the x – and y – axis so results are plotted for velocity profiles u and v respectively. One can see the dominant effects of velocity along u that present diagonally symmetric behavior within the corrugated cavity. It can further observe that all the boluses are originating at the top edge of the corrugated surface and expand gradually unless they reached at the mean position of the cavity. However, the behavior of velocity v along y – direction attained the more influence along the vertical direction. This is due to heat transfer and conduction is more influenced in the same vertical direction (see Fig. 9).

4.6. Effects of various heated lengths

Fig. 10 depicts the effects of various heated lengths on the flow field and temperature distributions inside the corrugated cavity through streamlines and isotherm plots, respectively. It can be noticed from Fig. 10(a)–(c) that the flow field tends to become stronger as the length of heated portion increases. The bullous are formed along the cold side wall due to boundary conditions. On the other hand, as the length of the heated portion is increased more fluid in the cavity is heated up. This is due to the fact that due to larger heated length more heat is transferred to the surrounding through convection. Is can be seen from Fig. 10(d)–(f) that the cavity starts to heat up in the middle portion which is due to the col side walls. Heat transfer rate along the (0, 0.05) to (1, 0.05) against the various length of heated portion can be seen from Fig. 11(a). The cup shaped profile trends are due to the corrugated wall. Moreover, it is noticed that with the increase in heated length the heat transfer along the specified path is decreased. The maximum heat transfer takes place at the boundary of the heated length. Fig. 11(b) satisfied the temperature boundary condition Eq. 8(a) which says that temperature at the hot corrugated wall is 1. Along the path (0.5, 0) to (0.5, 0.4) the temperature of fluid tends to decreased for different heated lengths. Moreover, at far away from the hot corrugated wall the temperature of fluid tends to increase due to increase in heated length (see Fig. 11(b)). The vertical velocity of fluid along (0.5, 0) to (0.5, 0.4) can be seen from Fig. 11(c). The zero velocity at the boundary satisfies the boundary condition Eq. 8(c). It is noted that, near heated corrugated wall, the velocity of the fluid tends to decrease due to increase in heated length. The maximum velocity is attained at the center along the path (0.5, 0) to (0.5, 0.4).

5. Conclusion

The natural convection flow and heat transfer characteristics of MHD fluid inside the corrugated rectangular cavity was investigated numerically using finite element method. Effects of wavelength parameter, Rayleigh number, Darcy number and Hartmann number was closely observed. It was found that both velocity flow and temperature fields tends to increase as the corrugation frequency and Rayleigh number are increased whereas it has inverse effect on the heat transfer rate. Nusselt number increased due to increase in wavelength parameter and Rayleigh number. Darcy and Hartmann number does not have significant effects on the temperature distribution. It is finally notice that, as the length of the heated portion is increased more fluid in the cavity is heated up.

Acknowledgement

Authors would like to acknowledge and express their gratitude to the United Arab Emirates University, Al Ain, UAE for providing the financial support with Grant No. 31S240-UPAR (2) 2016.

Conflict of interest

There is no actual or potential conflict of interest including any financial, personal or other relationships with other people or organizations.

References

[1] Adrian Bejan, Convection Heat Transfer, fourth ed., Wiley, New York, 2013.
[2] G. De Vahl Davis, Natural convection of air in a square cavity: a bench march numerical solution, Int. J. Numer. Meth. Fluids 3 (1983) 249–264.
[3] S. Ostrach, Natural convection in enclosures, J. Heat Transf. 110 (1988) 1175–1190.
[4] Khalil Khanafer, Kambiz Vafai, Marilyn Lightstone, Buoyancy-driven heat transfer enhancement in a two-dimensional enclosure utilizing nanofluids, Int. J. Heat Mass Transf. 46 (2003) 3639–3653.
[5] Raj Kamal Tiwari, Manab Kumar Das, Heat transfer augmentation in a two-sided lid-driven differentially heated square cavity utilizing nanofluids, Int. J. Heat Mass Transf. 50 (2007) 2002–2018.
[6] Eiyad Abu-Nada, Hakan F. Oztop, Effects of inclination angle on natural convection in enclosures filled with Cu-water nanofluid, Renew. Sustain. Energy Rev. 14 (2010) 629–641.
[7] Yasin Varol, Hakan F. Oztop, Ioan Pop, Entropy generation due to natural convection in non-uniformly heated porous isosceles triangular enclosures at different positions, Int. J. Heat Mass Transf. 52 (2009) 1193–1205.
[8] Tanmay Besak, G. Aravind, S. Roy, Visualization of heat flow due to natural convection within triangular cavities using Bejan's heat line concept, Int. J. Heat Mass Transf. 52 (2009) 2824–2833.
[9] Qiang Sun, Ioan Pop, Free convection in a triangle cavity filled with a porous medium saturated with nanofluids with flush mounted heater on the wall, Int. J. Therm. Sci. 50 (2011) 2141–2153.
[10] Khalil Khanafer, Kambiz Vafai, Marilyn Lightstone, Buoyancy-driven heat transfer enhancement in a two-dimensional enclosures utilizing nanofluids, Int. J. Heat Mass Transf. 46 (2003) 3639–3653.
[11] Eiyad Abu-Nada, Hakan F. Oztop, Effects of inclination angle on natural convection in enclosures filled with Cu-water nanofluid, Int. J. Heat Fluid Flow 30 (2009) 669–678.
[12] M. Sheikholeslami, M. Gorji-Bandpay, D.D. Ganji, Magnetic field effects on natural convection around a horizontal circular cylinder inside a square enclosure filled with nanofluids, Int. Commun. Heat Mass Transf. 39 (2011) 978–986.
[13] Yasin Varol, Hakan F. Oztop, Ioan Pop, Maximum density effects on buoyancy-driven convection in a porous trapezoidal cavity, Int. Commun. Heat Mass Transfer 37 (2010) 401–409.
[14] Mohammad Hemmat Esfe, Ali Akbar Abbasian Arani, Wei-Mon Yan, Hamidreza Ehteram, Alireza Aghaie, Masoud Afrand, Natural convection in a trapezoidal enclosure filled with carbon nanotubes-EG-water nanofluid, Int. J. Heat Mass Transf. 92 (2016) 76–82.
[15] Riwan Ul Haq, S. Naveed Kazmi, Toufik Mekkaoui, Thermal management of water based SWCNTs enclosed in a partially heated trapezoidal cavity via FEM, Int. J. Heat Mass Transf. 112 (2017) 972–982.
[16] Subrat Das, Yos Morsi, Natural convection inside dome shaped enclosures, Int. J. Numer. Meth. Heat Fluid Flow 12 (2002) 126–141.
[17] M.J. Uddin, M.S. Alam, M.M. Rahman, Natural convective heat transfer flow of nanofluids inside a quarter-circular enclosure using nonhomogeneous dynamic model, Arabian J. Sci. Eng. 42 (2017) 1883–1901.
[18] Myoung-Young Choi, Hyoung-Gwon Choi, A numerical study on the conjugate natural convection in a circular pipe containing water, J. Mech. Sci. Technol. 31 (2017) 3261–3269.
[19] Mohsen Sheikheleslami, Houman B. Rokni, Free convection of CuO-H_2O nanofluid in a curved porous enclosure using mesoscopic approach, Int. J. Hydrogen Energy 42 (2017) 14942–14949.
[20] Kamel Milani Shirvan, R. Ellahi, Mojtaba Mamourian, Mohammad Moghiman, Effects of wavy surface characteristics on natural convection heat transfer in a cosine corrugated square cavity filled with nanofluid, Int. J. Heat Mass Transf. 107 (2017) 1110–1118.
[21] M.M. Rahman, Hakan F. Oztop, A. Ahsan, J. Orfi, Natural convection effects on heat and mass transfer in a curvilinear triangular cavity, Int. J. Heat Mass Transf. 55 (2012) 6250–6259.
[22] M.M. Rahman, R. Saidur, S. Mekhilef, M. Borhan Uddin, A. Ahsan, Double-diffusive buoyancy induced flow in a triangular cavity with corrugated bottom wall: effects of geometrical parameters, Int. Commun. Heat Mass Transf. 45 (2013) 64–74.
[23] Muhammad Noman Hasan, Suvash C. Saha, Y.T. Gu, Unsteady natural convection within a differentially heated enclosure of sinusoidal corrugated side walls, Int. J. Heat Mass Transf. 55 (2012) 5696–5708.
[24] Mohammad Jafari, Mousa Farhadi, Kourosh Sedighi, Convection heat transfer SWCNT-nanofluid in a corrugated channel under pulsating velocity profile, Int. Commun. Heat Mass Transf. 67 (2015) 137–146.
[25] Z.H. Khan, M. Qasim, Riwan Ul Haq, Qasem M. Al-Mdallal, Closed form dual nature solutions of fluid flow and heat transfer over a stretching/shrinking sheet in a porous medium, Chin. J. Phys. 55 (2017) 1284–1293.
[26] X.B. Chen, P. Yu, Y. Sui, S.H. Winoto, H.T. Low, Natural convection in a cavity filled with porous layers on the top and bottom walls, Transp. Porous Media 78 (2009) 259–276.
[27] M.S. Astanina, M.A. Sheremet, J.C. Umavathi, Unsteady natural convection with temperature-dependent viscosity in a square cavity filled with a porous medium, Transp. Porous Media 110 (2015) 113–126.
[28] Tariq Javed, Z. Mehmood, Z. Abbas, Natural convection in square cavity filled with ferrofluid saturated porous medium in the presence of uniform magnetic field, Physica B 506 (2017) 122–132.
[29] P. Nithiarasu, K.N. Seetharamu, T. Sundararajan, Natural convective heat transfer in a fluid saturated variable porosity medium, Int. J. Heat Mass Transf. 40 (1997) 3955–3967.
[30] Aydin Misirlioglu, A. Cihat Baytas, Ioan Pop, Free convection in a wavy cavity filled with porous medium, Int. J. Heat Mass Transf. 48 (2005) 1840–1850.
[31] M.A. Sheremet, Ioan Pop, M.M. Rahman, Three-dimensional natural convection in a porous enclosure filled with a nanofluid using Buongiorno's mathematical model, Int. J. Heat Mass Transf. 82 (2015) 396–405.
[32] Tariq Javed, Ziafat Mehmood, Muhammad Arshad Siddiqui, Mixed convection in a triangular cavity permeated with micropolar nanofluid-saturated porous medium under the impact of MHD, J. Braz. Soc. Mech. Eng. Sci. 39 (2017) 3897–3909.
[33] M. Sheikholeslami, M. Shamlooei, Convective flow of nanofluid inside a lid driven porous cavity using CVFEM, Physica B 521 (2017) 239–250.
[34] Nirmalendu Biswas, Nirmal K. Manna, Enhanced convective heat transfer in lid-driven porous cavity with aspiration, Int. J. Heat Mass Transf. 114 (2017) 430–452.
[35] A. Shahzad, R. Ali, MHD flow of a non-Newtonian Power law fluid over a vertical stretching sheet with the convective boundary condition, Walailak J. Sci. Technol. (WJST) 10 (1) (2012) 43–56.
[36] A. Sokolov, R. Ali, S. Turek, An AFC-stabilized implicit finite element method for partial differential equations on evolving-in-time surfaces, J. Comput. Appl. Math. 289 (2014) 101–115.
[37] J. Ahmed, A. Shahzad, M. Khan, R. Ali, A note on convective heat transfer of an MHD Jeffrey fluid over a stretching sheet, AIP Adv. 5 (11) (2015) 117117.
[38] T. Aziz, F.M. Mahomed, A. Shahzad, R. Ali, Travelling wave solutions for the unsteady flow of a third grade fluid induced due to impulsive motion of flat porous plate embedded in a porous medium, J. Mech. 30 (05) (2015) 527–535.
[39] R. Ali, A. Shahzad, M. Khan, M. Ayub, Analytic and numerical solutions for axisymmetric flow with partial slip, Eng. Comput. 32 (1) (2016) 149–154.
[40] C. Taylor, P. Hood, A numerical solution of Navier-Stokes equations using finite element technique, Comput. Fluids 1 (1973) 73–89.
[41] P. Dachaumphai, Finite Element Method in Engineering, second ed., Chulalongkorn University Press, Bangkok, 1999.